Chapter 5

The Triply Bonded Al≡Sb Molecules: A Theoretical Prediction

Jia-Syun Lu, Ming-Chung Yang and Ming-Der Su

Additional information is available at the end of the chapter

http://dx.doi.org/10.5772/intechopen.78412

Abstract

The effect of substitution on the potential energy surfaces of RAl≡SbR (R = F, OH, H, CH_3, SiH_3, SiMe(Si*t*Bu$_3$)$_2$, Si*i*PrDis$_2$, Tbt, and Ar*) is investigated using density functional theories (M06-2X/Def2-TZVP, B3PW91/Def2-TZVP, and B3LYP/LANL2DZ + dp). The theoretical results demonstrated that all the triply bonded RAl≡SbR compounds with small substituents are unstable and can spontaneously rearrange to other doubly bonded isomers. That is, the smaller groups, such as R = F, OH, H, CH_3 and SiH_3, neither kinetically nor thermodynamically stabilize the triply bonded RAl≡SbR compounds. However, the triply bonded R′Al≡SbR′ molecules that feature bulkier substituents (R′ = SiMe(Si*t*Bu3)2, Si*i*PrDis2, Tbt, and Ar*) are found to possess the global minimum on the singlet potential energy surface and are both kinetically and thermodynamically stable. In particular, the bonding characters of the R′Al≡SbR′ species agree well with the valence-electron bonding model (model) as well as several theoretical analyses (the natural bond orbital, the natural resonance theory, and the charge decomposition analysis). That is to say, R′Al≡SbR′ molecules that feature groups are regarded as R′—Al⇇Sb—R′. Their theoretical evidence shows that both the electronic and the steric effects of bulkier substituent groups play a decisive role in making triply bonded R′Al≡SbR′ species synthetically accessible and isolable in a stable form.

Keywords: aluminum, antimony, group 13 elements, group 13 elements, triple bond

1. Introduction

The chemical synthesis and structural characterization of molecules that feature triple bonds [2] between heavier group 14 elements (E14 = Si, Ge, Sn and Pb) are of interest because of their interesting structural chemistry and their potential applications in organic and inorganic synthesis [1–10]. Although understanding of these RE14≡E14R molecules that feature heavier

group 14 atoms has increased during the last two decades, the understanding of the RE13≡E15R compounds, which are isoelectronic to acetylene from a valence electron viewpoint, is still limited. The reason for this limited knowledge of acetylene analogues, RE13≡E15R, could be due to the fact that there has been limited preparation and the isolation of these species in a stable form [11, 12]. Theoretical methods allow a theoretical design of the RE13≡E15R molecules to be made that increases understanding of their potential properties.

The III-V semiconductors that contain antimony have several important applications in optoelectronic devices that operate in the infrared region and in high-speed devices, which has prompted widespread studies of promising precursor systems for these materials [13]. In particular, the chemical synthesis and structural characterization of AlSb single-source precursors of the type R3Al-SbR′3 has attracted much attention, owing to their importance in CVD procedures [14], which is a developing industry for the production of thin films of the corresponding semiconducting materials [15]. As far as the authors are aware, only a handful of group 13 antimonides that contain Al—Sb σ-bonds have been discovered [16], No triply bonded RAl≡SbR species, which is isoelectronic to HC≡CH, has been reported both experimentally and theoretically.

Density functional theory (DFT) is sued to determine the structures, the kinetic stability and bonding properties of various RAl≡SbR triply bonded forms on the singlet ground state, in order to obtain a better understanding of aluminum≡antimony triple bonds. This work reports the possible existence of triply bonded RAl≡SbR molecules, from the viewpoint of the effect of substituents, using DFT [17]. That is, M06-2X/Def2-TZVP, B3PW91/Def2-TZVP

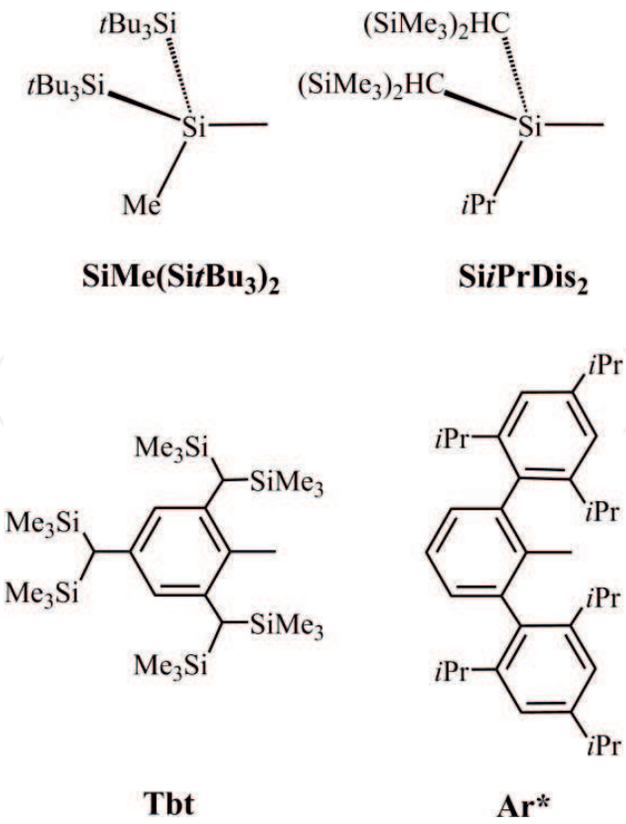

Scheme 1. Four bulky ligands, which are SiMe(Si*t*Bu$_3$)$_2$, Si*i*PrDis$_2$, Tbt, and Ar*.

and B3LYP/LANL2DZ + dp are used for small substituents (R = H, F, OH, CH_3, and SiH_3) and M06-2X/Def2-TZVP [18] for large substituents (R = SiMe(Si*t*Bu3)2, Si*i*PrDis2, Tbt, and Ar*; see **Scheme 1**) [19].

2. General considerations

The valence-bond bonding model is a well-known satisfactory method, which is an approximate theory to explain the electron pair or chemical bond by quantum mechanics, for predicting molecular geometries [20]. Two valence-bond bonding models (**Figure 1**) are thus used to interpret the bonding properties of triply bonded RAl≡SbR species. In model [1], the RAl≡SbR molecule is partitioned into two units: a singlet R—Al and a singlet R—Sb. In model [2], the RAl≡SbR compound is divided into two moieties: a triplet R—Al and a triplet R—Sb.

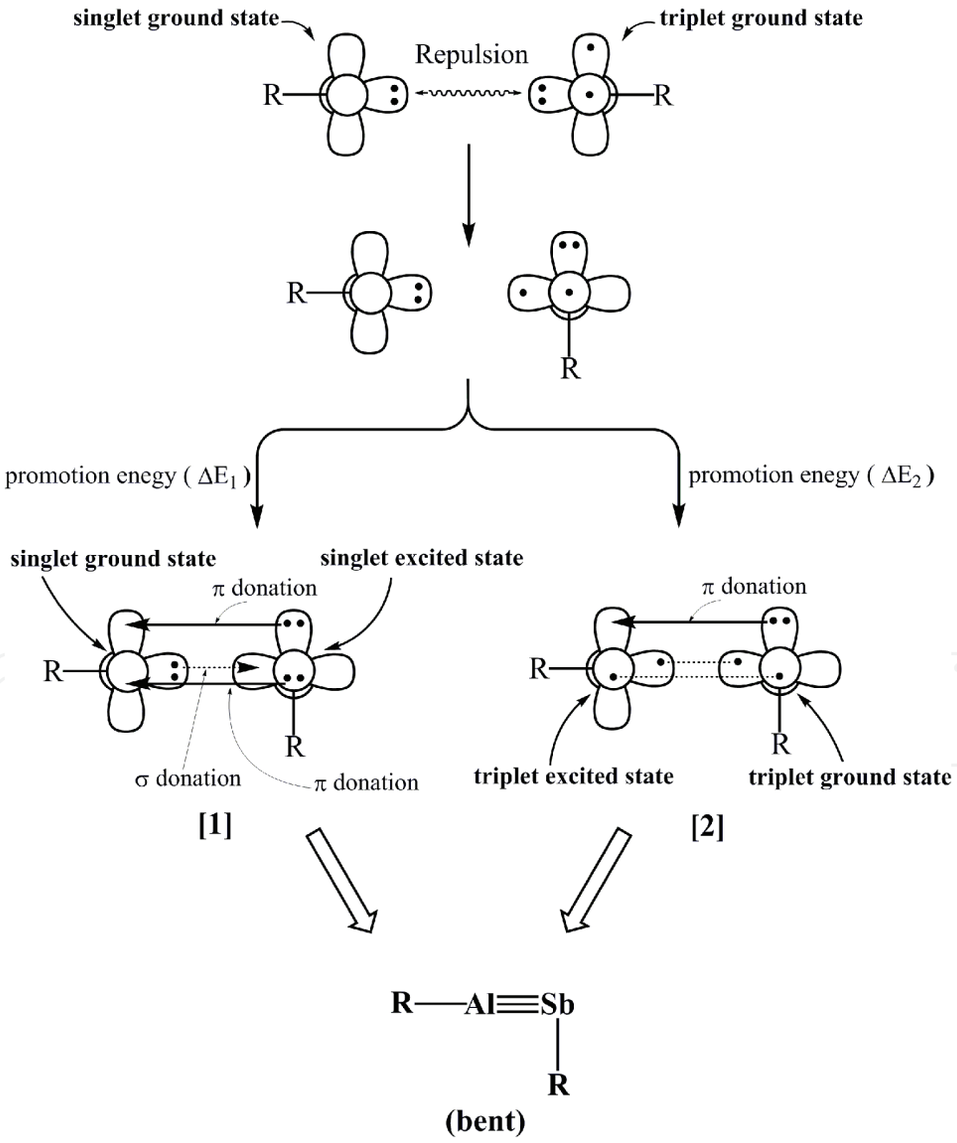

Figure 1. The valence-bond bonding models [1, 2] for the triply bonded RAl≡SbR molecule.

As a result, the choice of the bonding model that is used to explain the bonding characters of RAl≡SbR depends on the promotion energies ($\Delta E_{ST} = E_{triplet} - E_{singlet}$) of the R—Al and R—Sb fragments. According to current theoretical calculations (see below), it is known that R—Al occupies the singlet ground state, but R—Sb occupies the triplet ground state. In consequence, if the value of ΔE_{ST} for R—Al is much larger than that for R—Sb, the latter easily jumps to the singlet excited state. Hence, model [1] can be used to explain the bonding nature of the RAl≡SbR molecule. In contrast, if the value of ΔE_{ST} for R—Al is smaller than that for R—Sb, the former is readily promoted to the excited triplet state. Therefore, model [2] is used to interpret the bond constitutions of the RAl≡SbR compound.

Two points are worthy of note. The first is that since aluminum and antimony respectively belong to group 13 and group 15 and both elements have different atomic radii (covalent radii: 118 pm and 140 for Al and Sb, respectively) [20], the overlapping populations between Al and Sb should not be strong. The second is that the lone pairs of both aluminum and antimony feature the valence s character. This, in turn, makes the overlap integrals between the lone pair orbital and the pure p orbital small. These two factors mean that the triple bond between aluminum and antimony is weak, unlike the traditional triple bond in acetylene.

Bearing the above bonding analyses in mind, theoretical evidences are given in the following sections.

3. Results and discussion

3.1. Small ligands on substituted RAl≡SbR

Five small substituents (R = F, OH, H, CH_3 and SiH_3) are chosen, which include electronegative and electropositive groups, to determine their stability and bonding properties on the triply bonded RAl≡SbR molecules using the three types of DFT calculations (i.e., M06-2X/Def2-TZVP, B3PW91/Def2-TZVP and B3LYP/LANL2DZ + dp). **Figure 2** shows the potential energy surfaces of the intra-molecular 1,2-migration reactions for five triply bonded RAl≡SbR compounds that feature small substituents. That is to say, the triply bonded RAl≡SbR species can undergo a 1,2-shift to give either R2Al=Sb: or: Al=SbR2 doubly bonded isomers.

As seen in **Figure 2**, the three DFT computational results demonstrate that the triply bonded RAl≡SbR species that feature small substituents are all both kinetically and thermodynamically unstable on the intra-molecular 1,2-migration reaction potential energy surfaces. In other words, once the triply bonded RAl≡SbR with small substituents is formed, it can easily proceed along the 1,2-migration to give the thermodynamically stable doubly bonded isomer, either R2Al=Sb: or: Al=SbR2. The theoretical findings give strong evidence that the triply bonded RAl≡SbR molecules that feature the small ligands are highly unlikely to be detected experimentally.

Although current theoretical observations show that the formation of RAl≡SbR involving small ligands is not likely, some of their physical properties, which are shown in **Table 1**, must be theoretically determined in order to design much more stable aluminum≡antimony acetylene analogues.

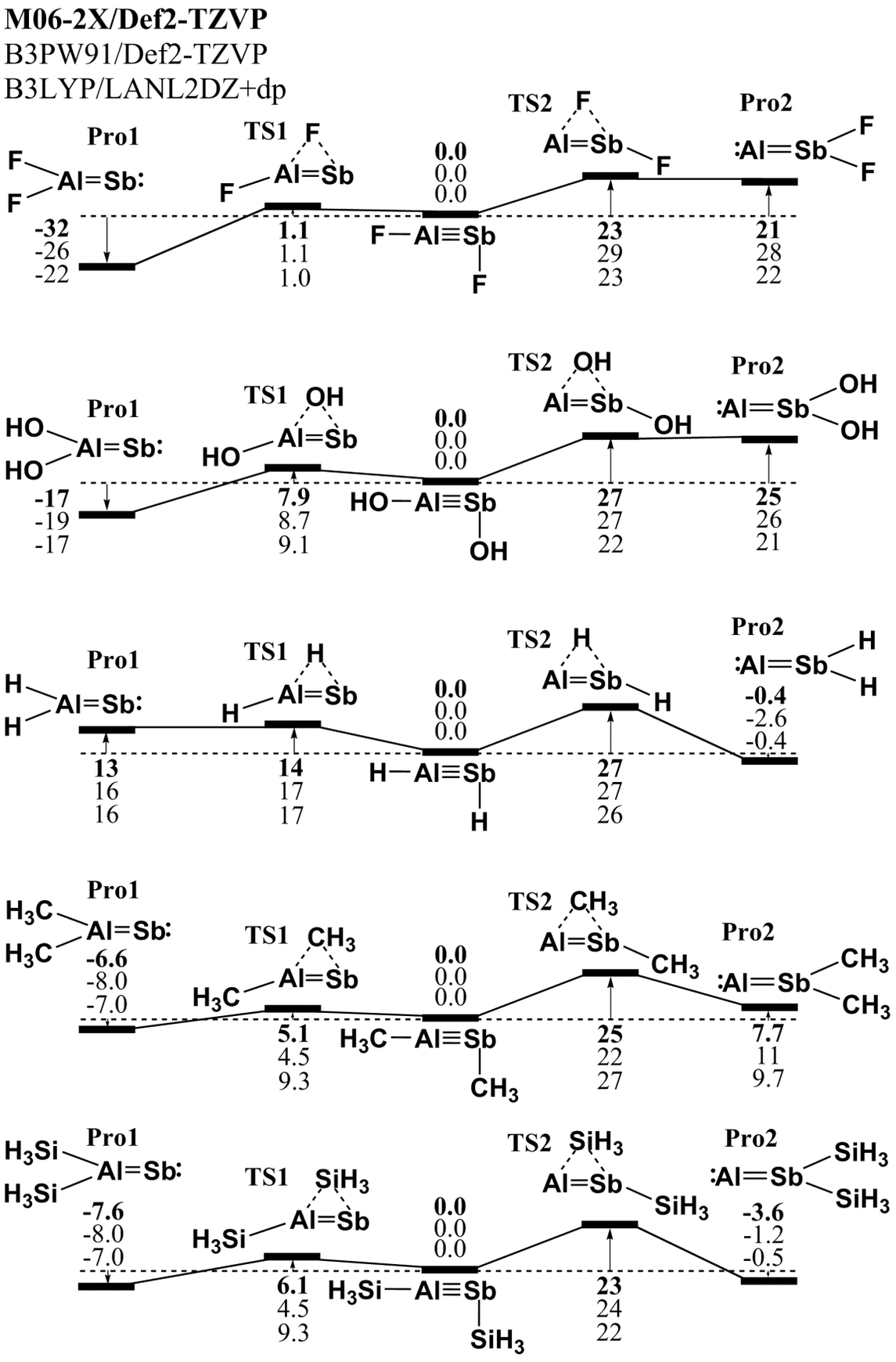

Figure 2. The 1,2-migration energy surfaces for RAl≡SbR (R = H, F, CH_3, OH, and SiH_3). These relative Gibbs free energies (kcal/mol) are computed at the M06-2X/Def2-TZVP, B3PW91/Def2-TZVP, and B3LYP/LANL2DZ + dp levels of theory.

R	F	OH	H	CH_3	SiH_3
AlαSb (Å)	2.528 (2.536) [2.556]	2.531 (2.518) [2.565]	2.388 (2.397) [2.436]	2.466 (2.462) [2.499]	2.539 (2.524) [2.560]
∠R-Al-Sb (°)	176.8 (176.2) [179.2]	173.4 (172.0) [176.5]	170.7 (167.6) [167.6]	177.7 (173.8) [173.2]	176.8 (176.2) [179.7]
∠Al-Sb-R (°)	88.86 (88.07) [88.53]	86.55 (86.13) [90.43]	82.25 (84.42) [86.43]	94.46 (96.42) [96.75]	88.86 (88.07) [88.53]
∠R-Sb-Al-R (°)	179.9 (179.9) [180.0]	179.7 (176.9) [178.6]	180.0 (180.0) [180.0]	179.6 (179.9) [178.2]	179.9 (179.9) [180.0]
Q_{Al}[1]	0.5201 (0.495) [0.715]	0.418 (0.401) [0.469]	0.164 (0.161) [0.414]	0.291 (0.262) [0.282]	0.208 (0.219) [0.193]
Q_{Sb}[2]	0.329 (0.277) [0.217]	0.196 (0.136) [0.119]	−0.134 (−0.107) [-0.032]	−0.054 (−0.018) [−0.134]	−0.198 (−0.100) [−0.179]
ΔE_{ST} for Al-R (kcal/mol)[3]	79.78 (71.44) [73.78]	72.05 (65.86) [67.75]	43.73 (40.25) [40.80]	48.75 (42.38) [45.00]	32.87 (29.08) [31.97]
ΔE_{ST} for Sb-R (kcal/mol)[4]	−32.40 (−28.88) [−27.52]	−25.88 (−21.16) [−20.04]	−33.35 (−29.42) [−27.91]	−31.52 (−27.31) [−26.00]	−30.78 (−25.61) [−25.21]
HOMO-LUMO (kcal/mol)	165.5 (168.4) [167.2]	159.8 (140.1) [145.2]	257.6 (205.2) [277.6]	146.4 (123.3) [129.2]	172.2 (179.5) [177.9]
BE (kcal/mol)[5]	25.82 (32.05) [27.43]	22.77 (27.32) [21.96]	55.28 (64.05) [56.79]	42.23 (51.72) [46.41]	61.00 (67.80) [57.43]
WBI[6]	1.483 (1.556) [1.560]	1.474 (1.550) [1.555]	1.754 (1.799) [1.779]	1.659 (1.714) [1.733]	1.581 (1.596) [1.637]

[1]The charge density on the Al element.
[2]The charge density on the Sb element.
[3]ΔE_{ST} = E(triplet state for R—Al) − E(singlet state for R—Sb).
[4]ΔE_{ST} = E(triplet state for R—Al) − E(singlet state for R—Sb).
[5]BE = E(singlet state for R—Al) + E(triplet state for R—Sb) − E(singlet state for RAl≡SbR).
[6]The Wiberg bond index (WBI) for the Al≡Sb bond: see Ref. [22].

Table 1. The key geometrical parameters, the singlet-triplet energy splitting (ΔE_{ST}), the natural charge densities (QAl and QSb), the binding energies (BE), the HOMO-LUMO energy gaps, and the Wiberg bond index (WBI) for RAl≡SbR using the M06-2X/Def2-TZVP, B3PW91/Def2-TZVP (in round brackets) and B3LYP/LANL2DZ + dp (in square brackets) levels of theory.

As seen in **Table 1**, the three DFT computational results predict that the Al≡Sb triple bond distance (Å) is in the ranges 2.388–2.539 (M06-2X/Def2-TZVP), 2.397–2.536 (B3PW91/Def2-TZVP) and 2.436–2.565 (B3LYP/LANL2DZ + dp). **Table 1** also shows that all of the geometrical

http://dx.doi.org/10.5772/intechopen.78412

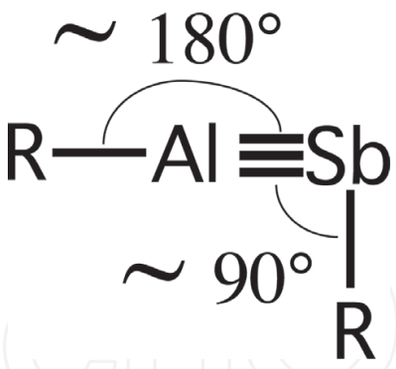

Scheme 2. The geometrical structure of RAl≡SbR with the small substituent, R.

structures of RAl≡SbR adopt the bent form, as demonstrated in **Scheme 2**. That is, ∠R—Al—Sb ≈ 180.0° and ∠Al—Sb—R ≈ 90.0°. The reason for this vertical angle at the Sb center can be ascribed to the relativistic effect, as discussed previously [21]. The three DFT calculations shown in **Table 1** all indicate that the electronic ground states for R—Al and the R—Sb fragments are singlet and triplet, respectively. In particular, all of the DFT results shown in **Table 1** show that most of the singlet-triplet energy splitting (ΔE_{ST}) of R-Al is larger than that of the corresponding R—Sb. This strongly implies that the bonding characters of the triply bonded RAl≡SbR species that feature small substituents are better described by model [1], as shown in **Figure 1**. In other words, the triple bond consists of one donor-acceptor σ bond and two donor-acceptor π bonds, which are schematically represented as R—Al⇆Sb—R. As previously mentioned, since the lone pair orbitals of both the R-Al and the R-Sb fragments feature the valence s character, their overlapping populations between the lone orbital and the valence p orbital should be smaller. Indeed, the supporting evidence from **Table 1** shows that all bond orders for the RAl≡SbR species are estimated to be less than 2.0 (WBI = 1.474–1.799), which is less than the bond order for the C≡C triple bond in acetylene (WBI = 2.99).

In brief, the three DFT calculations shown in this work show that irrespective of their electronegativity, the triply bonded RAl≡SbR molecules that feature small ligands are highly unlikely to exist, even in the low-temperature matrices. In particular, the bond orders of these Al≡Sb triple bonds are theoretically predicted to be a weak double bond, rather than a triple bond.

3.2. Large ligands on substituted R′Al≡SbR′

Three bulky groups were then used to search for kinetically stable triple-bonded R′Al≡SbR′ molecules: R′(=SiMe(Si*t*Bu3)2, Si*i*PrDis2, Tbt, and Ar*) [19]. These are shown in **Scheme 1**. It is known that London dispersion (nonvalent interactions) plays a prominent role in both chemical and physical properties of inorganic molecules [23]. As a result, the dispersion-corrected M06-2X/Def2-TZVP method is used in the present study to investigate the behaviors of the triply bonded R′Al≡SbR′ compounds bearing bulky substituents. Similarly to the cases for small ligands on substituted RAl≡SbR, the dispersion-corrected M06-2X/Def2-TZVP level of theory is used to determine the potential energy surfaces for the intra-molecular 1,2-migration

reactions of R′Al≡SbR′, as shown in **Scheme 3**. The computed relative energies are listed in **Table 2**. The reaction enthalpies for both the 1,2-shift reactions (R′Al≡SbR′ → R2′Al=Sb and R′Al≡SbR′ → R2′Sb=Al) are apparently too high. They are estimated to be at least 80 kcal/mol. The reason that both doubly bonded R2′Al=Sb and R2′Sb=Al isomers occupy such high energy points is simply because two bulky groups can cause steric overcrowding. As a consequence, the theoretical findings strongly suggest that the triply bonded R′Al≡SbR′, which is attached by two bulkier substituents, is kinetically stabilized.

Table 2 shows that the Al≡Sb triple bond distance is predicted to be 2.422–2.477 Å. Since no experimental results for the Al≡Sb triple bond length have been reported, these values are estimates. These theoretical calculations also show that the geometrical structures of R′Al≡SbR′ molecules that feature bulky groups adopt a bent structure; i.e., ∠R′—Al—Sb ≈ 160.0° and ∠Al—Sb—R′ ≈ 120.0°. As stated previously, the triply bonded R′Al≡SbR′ species feature this bent geometry because of the relativistic effect [23].

In addition, the bonding energy (BE) that is shown in **Table 2** shows that the central aluminum and antimony atoms in the substituted R′Al≡SbR′ compounds are strongly bonded, since the

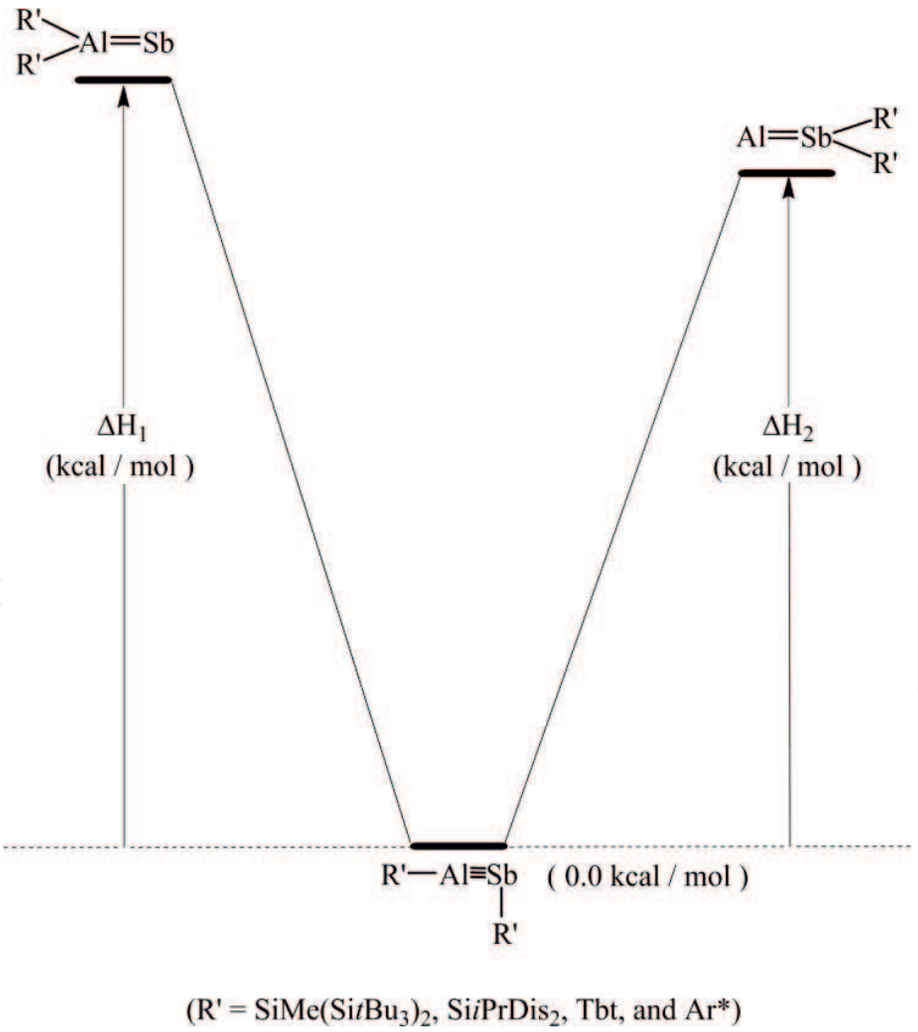

Scheme 3. The qualitative potential energy surface of the R′Al≡SbR′ isomers with the bulky substituent, R′.

R′	SiMe(Si*t*Bu$_3$)$_2$	Si*i*PrDis$_2$	Tbt	Ar*
Al≡Sb (Å)	2.463	2.422	2.477	2.447
∠R′—Al—Sb (°)	157.6	152.0	161.3	165.0
∠Al—Sb—R′ (°)	126.5	123.6	122.2	124.6
∠R′—Al—Sb—R′ (°)	173.5	172.9	167.2	166.0
Q_{Al}[1]	0.619	0.637	1.008	1.027
Q_{Sb}[2]	−0.387	−0.492	−0.025	−0.114
ΔE_{ST} for Al—R′ (kcal/mol)[3]	28.89	27.30	42.50	40.21
ΔE_{ST} for Sb—R′ (kcal/mol)[4]	−16.89	−24.80	−30.51	−15.92
HOMO-LUMO (kcal/mol)	53.56	60.07	56.08	56.68
BE (kcal/mol)[5]	71.29	72.97	87.43	74.33
ΔH_1 (kcal/mol)[6]	94.23	84.67	92.12	82.68
ΔH_2 (kcal/mol)[6]	83.15	84.08	80.01	88.19
WBI[7]	2.174	2.181	2.072	2.016

[1]The charge density on the Al element.
[2]The charge density on the Sb element.
[3]ΔE_{ST} (kcal mol^{-1}) = E(triplet state for R′—Al) − E(singlet state for R′—Al).
[4]ΔE_{ST} (kcal mol^{-1}) = E(triplet state for R′—Sb) − E(singlet state for R′—Sb).
[5]BE (kcal mol^{-1}) = E(triplet state for R′—Al) + E(triplet state for R′—Sb) − E(singlet for R′Al≡SbR′).
[6]See **Scheme 3**.
[7]The Wiberg bond index (WBI) for the Al*α*Sb bond: see Ref. [22].
See also **Scheme 3**.

Table 2. The key geometrical parameters, the singlet-triplet energy splitting (ΔE_{ST}), the natural charge densities (QAl and QSb), the binding energies (BE), the HOMO-LUMO energy gaps, reaction enthalpies, and the Wiberg bond index (WBI) for R′Al≡SbR′ at the dispersion-corrected M06-2X/Def2-TZVP level of theory.

BE values are in the range 71–97 kcal/mol for R′ = SiMe(Si*t*Bu3)2, Si*i*PrDis2, Tbt, and Ar*. **Table 2** also shows that the modulus ΔE_{ST} (kcal/mol) for Al—R′ and Sb—R′ fragments are predicted to be 43–27 and 31–16. These theoretical values allow two interpretations. Firstly, even when attached by bulkier groups, it is theoretically verified that both the Al—R′ and the Sb—R′ units occupy the ground singlet state and the ground triplet state, respectively. Since the ΔE_{ST} values for Al—R′ are so small (compared with those for Al—R, as shown in **Table 1**), model [2] in **Figure 1** is most suitable to interpret the triple bonding characters in the R′Al≡SbR′ species that feature bulky substituents. As schematically shown in **Figure 1**, the nature of the Al≡Sb triple bond can be considered as one conventional σ bond, one conventional π bond and one donor-acceptor π bond. That is, R′—Al⇇Sb—R′. It is worthy of note that two factors affect the overlapping populations between the central Al and Sb elements. The first is that the lone pair orbital of the Sb—R′ moiety features the valence s character. This, in turn, renders the overlap population between the pure p orbital of Al and the lone pair orbital of Sb very small. The other is that the sizes of the valence p orbitals for Al and Sb are quite different, since they belong to different rows of the periodic table having different principal quantum numbers. As a result, the triple bond in R′Al≡SbR′ molecules that feature

bulky substituents is predicted to be quite weak. Indeed, the theoretical evidences given in **Table 2** shows that the bond order is a little bit higher than 2.0 (WBI ≈ 2.17, 2.18, 2.07 and 2.02 for R′ = SiMe(Si*t*Bu3)2, Si*i*PrDis2, Tbt, and Ar*, respectively). The bond order for the conventional C≡C bond in acetylene is estimated to be 2.99.

Besides these, Dapprich and Frenking developed a useful method [24], which is called the introduced charge decomposition analysis (CDA), from which one may analyze donor-acceptor interactions of a A-B molecule. From CDA, one may obtain three parts. The first part is the number of electrons donated from the R′—Al unit to the R′—Sb monomer, which can be considered as (R′—Al) → (R′—Sb). The second part is the number of electrons back donated from the R′—Sb component to the R′—Al moiety, which can be represented as (R′—Al) ← (R′—Sb). The third part is the repulsive interactions between (R′—Al) and (R′—Sb), which can be described as (R′—Al) ↔ (R′—Sb). The CDA results about the (SiMe(Si*t*Bu$_3$)$_2$)Al≡Sb(SiMe(Si*t*Bu$_3$)$_2$) molecule based on the dispersion-corrected M06-2X/Def2-TZVP method are given in **Table 3**. As seen in **Table 3**, for the (R′—Sb) fragment, its largest contribution is No. 267 (HOMO) orbital, displaying that a R′—Sb component donates electrons to a R′—Ga unit mainly through the HOMO orbital. In consequence, the net amount of electron transfer is estimated to be −0.207, implying that the R′—Sb part donates more electrons to the R′—Al moiety. This theoretical finding agrees well with the valence-electron bonding model shown in **Figure 1** (i.e., model [2]). Namely, the bonding character of R′Al≡SbR′ can be recognized as R′Al⇇SbR′.

	Orbital	Occupancy	A	B	A-B	W
	257	2.000000	0.000897	0.000398	0.000499	0.000052
	258	2.000000	−0.000691	−0.000223	−0.000469	−0.003158
	259	2.000000	0.000003	0.000212	−0.000209	−0.000135
	260	2.000000	−0.000574	0.001495	−0.002069	−0.003430
	261	2.000000	0.000322	0.000997	−0.000676	−0.003797
	262	2.000000	0.000333	0.000068	−0.002466	−0.012549
	263	2.000000	0.000927	0.007097	0.000859	0.000836
	264	2.000000	0.001417	0.031682	−0.003680	−0.003811
	265	2.000000	0.005618	0.033540	−0.057513	−0.129159
	266	2.000000	0.016174	0.031540	−0.017366	0.011841
HOMO	267	2.000000	−0.000521	0.063131	−0.032203	−0.047961
LUMO	268	0.000000	0.000000	0.000000	0.000000	0.000000
	269	0.000000	0.000000	0.000000	0.000000	0.000000
Sum[a]		534.000000	0.043071	0.250110	−0.207039	−0.099090

For clearness, only list the X, Y, and W terms for HOMO(no.267)-11 ∼ LUMO+2.
[a]Summation of contributions from all unoccupied and occupied orbitals.

Table 3. The charge decomposition analysis (CDA) for R′Al≡SbR′ (R′ = SiMe(Si*t*Bu$_3$)$_2$) system based on M06-2X orbitals, where a is the number of electrons donating from R′—Al unit to R′—Sb unit, B is the number of electrons donating from R′-Sb moiety to R′-Al moiety and W is the number of electrons involved in repulsive polarization.

http://dx.doi.org/10.5772/intechopen.78412

The bonding characters of the Al≡Sb triple bond in R′Al≡SbR′ molecules were examined using the natural bond orbital (NBO) [22] and the natural resonance theory (NRT) [25] analysis, whose results are given in **Table 4**, are used to determine the bonding properties. For instance, **Table 4** shows that for (SiMe(Si*t*Bu3)2)Al≡Sb(SiMe(Si*t*Bu3)2), the NBO model shows that the Al-Sb σ bonding orbital contains about 23% natural Al orbitals and 77% natural Sb orbitals. Also, the Al≡Sb π bonding orbital contains averagely about 25% natural Al orbitals and 75% natural Sb orbitals (**Figure 3**). These values give strong evidence that the Al≡Sb π bond is polarized. **Table 4** also shows that the Al≡Sb π bonding interaction: $\pi_{\perp}$(Al≡Sb) = 0.529 (3s3p$^{1.98}$)Al + 0.849(5s5p$^{12.43}$)Sb and $\pi_{\parallel}$(Al≡Sb) = 0.475(3s3p$^{99.99}$)Al + 0.880(5s5p$^{99.99}$)Sb, which again implies that the predominant bonding interaction between the Al—R and the Sb—R moieties originates from 3p(Al) ← 5p(Sb) donation. In other words, the electron deficiency on Al and the π bond polarity are partially balanced by the donation of the Sb lone pair to the empty Al p orbital (**Figure 3**). **Table 4** also shows that, on the basis of the NRT analyses of the electron density for (SiMe(Si*t*Bu3)2)Al≡Sb(SiMe(Si*t*Bu3)2), its Al≡Sb triple bond has a greater

R′Al≡SbR′	WBI	NBO analysis			NRT analysis	
		Occupancy	Hybridization	Polarization	Total/covalent/ionic	Resonance weight
R′ = SiMe(Si*t*Bu$_3$)$_2$	2.17	σ: 1.91	σ: 0.4799 Al (sp$^{3.23}$) + 0.8773 Sb (sp$^{0.60}$)	23.03% (Al) 76.97% (Sb)	2.06/1.25/0.81	Al—Sb: 10.84% Al〓Sb: 71.95% Al≡Sb: 17.21%
		$\pi_{\perp}$: 1.81	$\pi_{\perp}$: 0.5288 Al (sp$^{1.98}$) + 0.8487 Sb (sp$^{12.43}$)	27.96% (Al) 72.04% (Sb)		
		$\pi_{\parallel}$: 1.89	$\pi_{\parallel}$: 0.4753 Al (sp$^{99.99}$) + 0.8798 Sb (sp$^{99.99}$)	22.59% (Al) 77.41% (Sb)		
R′ = Si*i*PrDis$_2$	2.18	σ: 1.91	σ: 0.5525 Al (sp$^{1.71}$) + 0.8335 Sb (sp$^{1.15}$)	30.53% (Al) 69.47% (Sb)	2.48/1.29/1.19	Al—Sb: 10.63% Al〓Sb: 75.53% Al≡Sb: 13.84%
		$\pi_{\perp}$: 1.86	$\pi_{\perp}$: 0.4723 Al (sp$^{3.67}$) + 0.8815 Sb (sp$^{3.68}$)	22.30% (Al) 77.70% (Sb)		
		$\pi_{\parallel}$: 1.89	$\pi_{\parallel}$: 0.4476 Al (sp$^{99.99}$) + 0.8943 Sb (sp$^{99.99}$)	20.03% (Al) 79.97% (Sb)		
R′ = Tbt	2.07	σ: 1.95	σ: 0.6923 Al (sp$^{0.18}$) + 0.7216 Sb (sp$^{12.38}$)	47.93% (Al) 52.07% (Sb)	2.22/1.41/0.82	Al—Sb: 5.89% Al〓Sb: 65.89% Al≡Sb: 28.22%
		$\pi_{\perp}$: 1.88	$\pi_{\perp}$: 0.4488 Al (sp$^{47.14}$) + 0.8936 Sb (sp$^{99.99}$)	20.14% (Al) 79.86% (Sb)		
		$\pi_{\parallel}$: 1.91	$\pi_{\parallel}$: 0.4772 Al (sp$^{99.99}$) + 0.8788 Sb (sp$^{99.99}$)	22.78% (Al) 77.22% (Sb)		
R′ = Ar*	2.02	σ: 1.96	σ: 0.6946 Al (sp$^{0.16}$) + 0.7194 Sb (sp$^{18.14}$)	48.25% (Al) 51.75% (Sb)	2.01/1.44/0.57	Al—Sb: 11.37% Al〓Sb: 76.76% Al≡Sb: 11.87%
		$\pi_{\perp}$: 1.83	$\pi_{\perp}$: 0.4543 Al (sp$^{99.99}$) + 0.8908 Sb (sp$^{40.30}$)	20.64% (Al) 79.36% (Sb)		
		$\pi_{\parallel}$: 1.92	$\pi_{\parallel}$: 0.4266 Al (sp$^{99.99}$) + 0.9044 Sb (sp$^{99.99}$)	18.20% (Al) 81.80% (Sb)		

Table 4. The natural bond orbital (NBO), the natural resonance theory (NRT) analysis, and Wiberg bond index (WBI) for R′Al≡SbR′ molecules that feature ligands (R′ = SiMe(Si*t*Bu$_3$)$_2$, Si*i*PrDis$_2$, and NHC) at the dispersion-corrected M06-2X/Def2-TZVP level of theory.

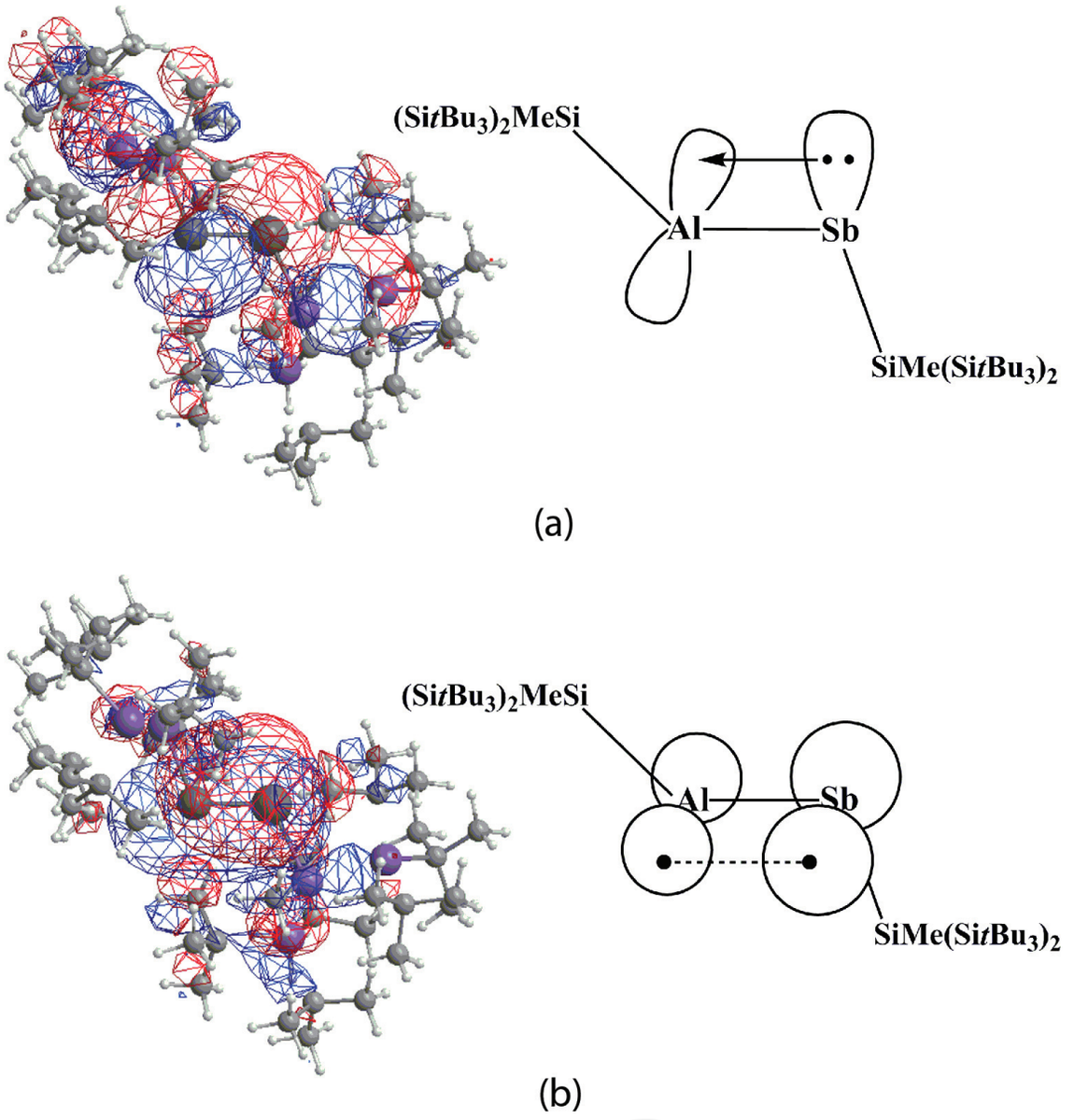

Figure 3. The natural Al≡Sb π bonding orbitals ((i) and (ii)) for (SiMe(Si*t*Bu$_3$)$_2$)Al≡Sb(SiMe(Si*t*Bu$_3$)$_2$). Also, see **Figure 1**. (i) $\pi_{\perp}$, (ii) $\pi_{\parallel}$.

covalent character, as shown by the greater covalent part of the NRT bond order (1.25), compared to its ionic part (0.81). The reason for this may be due to the fact that the difference between the electronegativity values for the Al and Sb elements is small (Al: 1.5 and Sb: 1.8) [26].

4. Conclusion

This study uses DFT computations to theoretically design substituted RAl≡SbR molecules that feature the Al≡Sb triple bond, that are stable from the kinetic viewpoint. The theoretical observations show that only bulky substituents (R′) can significantly stabilize the triply

bonded R′Al≡SbR′ compounds, and not small substituents. The theoretical findings also show that the bonding characters of the R′Al≡SbR′ species that feature bulky groups can be represented as R′—Al⇆Sb—R′. That is to say, the R′Al≡SbR′ species contains a conventional σ bond, a conventional π bond and a donor-acceptor π bond. However, due to the poor overlapping populations between the Al and Sb elements, which is due to the different atomic sizes of the two elements and the nature of overlapping bonding orbitals, the Al≡Sb triple bond is very weak. The theoretical results also give strong evidence that the geometrical structures of the R′Al≡SbR′ species adopt a bent conformation with a nearly perpendicular angle at the antimony center.

Acknowledgements

The authors are grateful to the National Center for High-Performance Computing of Taiwan for generous amounts of computing time, and the Ministry of Science and Technology of Taiwan for the financial support.

Author details

Jia-Syun Lu[1], Ming-Chung Yang[1] and Ming-Der Su[1,2]*

*Address all correspondence to: midesu@mail.ncyu.edu.tw

1 Department of Applied Chemistry, National Chiayi University, Chiayi, Taiwan

2 Department of Medicinal and Applied Chemistry, Kaohsiung Medical University, Kaohsiung, Taiwan

References

[1] Fischer RC, Power PP. π-Bonding and the lone pair effect in multiple bonds involving heavier main group elements: Developments in the new millennium. Chemical Reviews. 2010;**110**:3877-3923. DOI: 10.1021/cr100133q

[2] Danovich D, Bino A, Shaik S. Formation of carbon–carbon triply bonded molecules from two free carbyne radicals via a conical intersection. Journal of Physical Chemistry Letters. 2013;**4**:58-64. DOI: 10.1021/jz3016765

[3] Sasamori T, Hironaka K, Sugiyama T, Takagi N, Nagase S, Hosoi Y, Furukawa Y, Tokitoh N. Synthesis and reactions of a stable 1,2-diaryl-1,2-dibromodisilene: A precursor for substituted disilenes and a 1,2-diaryldisilyne. Journal of the American Chemical Society. 2008;**130**:13856-13857. DOI: 10.1021/ja8061002.

[4] Spikes GH, Power PP. Lewis base induced tuning of the Ge–Ge bond order in a "digermyne". Chemical Communications. 2007;**1**:85-87. DOI: 10.1039/B612202G

[5] Phillips AD, Wright RJ, Olmstead MM, Synthesis PPP. Characterization of 2,6-$Dipp_2$-$H_3C_6SnSnC_6H_3$-2,6-$Dipp_2$ (Dipp = C_6H_3-2,6-Pr^i_2): A tin analogue of an alkyne. Journal of the American Chemical Society. 2002;**124**:5930-5931. DOI: 10.1021/ja0257164

[6] Pu L, Twamley B, Power PP. Synthesis and characterization of 2,6-$Trip_2H_3C_6PbPbC_6H_3$-2,6-$Trip_2$ (trip=C_6H_2-2,4,6-i-Pr_3): A stable heavier group 14 element analogue of an alkyne. Journal of the American Chemical Society. 2000;**122**:3524-3525. DOI: 10.1021/ja993346m

[7] Lühmann N, Müller T. A compound with a Si–C triple bond. Angewandte Chemie, International Edition. 2010;**49**:10042-10044. DOI: 10.1002/anie.201005149

[8] Wu P-C, Su M-D. Theoretical designs for germaacetylene (RC≡GeR'): A new target for synthesis. Dalton Transactions. 2011;**40**:4253-4259. DOI: 10.1039/C0DT00800A

[9] Wu P-C, Su M-D. Triply bonded stannaacetylene (RC≡SnR): Theoretical designs and characterization. Inorganic Chemistry. 2011;**50**:6814-6822. DOI: 10.1021/ic200930v

[10] Wu P-C, Su M-D. A new target for synthesis of triply bonded plumbacetylene (RC≡PbR): A theoretical design. Organometallics. 2011;**30**:3293-3301. DOI: 10.1021/om2000234

[11] Paetzold P. Boron-nitrogen analogues of cyclobutadiene, benzene and cyclooctatetraene. Phosphorus, Sulfur, and Silicon. 1994;**93-94**:39-50. DOI: 10.1080/10426509408021797

[12] Wright RJ, Phillips AD, Allen TL, Fink WH, Power PP. Synthesis and characterization of the monomeric imides Ar′MNAr′′ (M = Ga or in; Ar′ or Ar′′ = terphenyl ligands) with two-coordinate gallium and indium. Journal of the American Chemical Society. 2003;**125**:1694-1695. DOI: 10.1021/ja029422u

[13] Gardiner MG, Raston CL. Advances in the chemistry of Lewis base adducts of alane and gallane. Coordination Chemistry Reviews. 1997;**166**:1-34. DOI: 10.1016/S0010-8545(97)00002-7

[14] Grovenor CRM. Microelectronic Materials. Philadelphia, PA: Adam Hilger; 1989

[15] Park HY, Wessels A, Roesky HW, Schulz S. First approach to an AlSb layer from the single source precursors $[Et_2AlSb(SiMe_3)_2]_2$ and $[^iBu_2AlSb(SiMe_3)_2]_2$. Chemical Vapor Deposition. 1999;**5**:179-184. DOI: 10.1002/(SICI)1521-3862(199908)5:4<179::AID CVDE179>3.0.CO;2-6

[16] Schulz S, Kuczkowski A, Nieger M. Synthesis and X-ray structures of all-alkyl-substituted AlSb ring compounds. Organometallics. 2000;**19**:699-702. DOI: 10.1021/om990795m

[17] Kuczkowski A, Schulz S, Nieger M, Schreiner PR. Experimental and Computational Studies of R_3Al-ER′$_3$ (E = P, As, Sb, Bi; R = Et, *t*-Bu; R′ = $SiMe_3$, *i*-Pr) Donor-Acceptor Complexes: Role of the Central Pnictine and the Substituents on the Structure and Stability of Alane Adducts. Organometallics. 2002;**21**:1408-1419. DOI: 10.1021/om0200205

[18] Zhao Y, Truhlar DG. Density functionals with broad applicability in chemistry. Accounts of Chemical Research. 2008;**41**:157-167. DOI: 10.1021/ar700111a

[19] Takagi N, Nagase S. Substituent effects on germanium−germanium and tin−tin triple bonds. Organometallics. 2001;**20**:5498-5500. DOI: 10.1021/om010669u

[20] Ebbing DD, Gammon SD. General Chemistry. New York: Brooks/Cole; 2015. Chap. 9

[21] Reed AE, Curtiss LA, Weinhold F. Intermolecular interactions from a natural bond orbital, donor-acceptor viewpoint. Chemical Reviews. 1998;**88**:899-926. DOI: 10.1021/cr00088a005

[22] Pyykkö P. Strong closed-shell interactions in inorganic chemistry. Chemical Reviews. 1997;**97**:597-636. DOI: 10.1021/cr940396v

[23] Liptrot DJ, Power PP. London dispersion forces in sterically crowded inorganic and organometallic molecules. Nature Reviews Chemistry. 2017;**1**:4-16. DOI: 10.1038/s41570-016-0004

[24] Dapprich S, Frenking G. Investigation of donor-acceptor interactions: A charge decomposition analysis using fragment molecular orbitals. The Journal of Physical Chemistry. 1995; **99**:9352-9362. DOI: 10.1021/j100023a009

[25] Glendening ED, Badenhoop JK, Weinhold F. Natural resonance theory. III. Chemical applications. Journal of Computational Chemistry. 1998;**19**:628-646. DOI: 10.1002/(SICI)1096-987X(19980430)19:6<628::AID-JCC5>3.0.CO;2-T

[26] Huheey JE, Keiter EA, Keiter RL. Inorganic Chemistry: Principles of Structure and Reactivity. 4th ed. New York, USA: Harper Collins; 1993. p. 246

IntechOpen